NeuroImage 220 (2020) 117084

Contents lists available at ScienceDirect

NeuroImage

journal homepage: www.elsevier.com/locate/neuroimage

Distinct patterns of surround modulation in V1 and hMT+

Gorkem Er [a,1], Zahide Pamir [a,1,2,*], Huseyin Boyaci [a,b,c]

[a] A.S. Brain Research Center, National Magnetic Resonance Research Center (UMRAM), Neuroscience Graduate Program, Bilkent University, Ankara, Turkey
[b] Department of Psychology, Bilkent University, Ankara, Turkey
[c] Department of Psychology, JL Gießen University, Gießen, Germany

ARTICLE INFO

Keywords:
Surround modulation
Surround suppression
Surround facilitation
Motion perception
Primary visual cortex
Middle temporal complex

ABSTRACT

Modulation of a neuron's responses by the stimuli presented outside of its classical receptive field is ubiquitous in the visual system. This "surround modulation" mechanism is believed to be critical for efficient processing and leads to many well-known perceptual effects. The details of surround modulation, however, are still not fully understood. One of the open questions is related to the differences in surround modulation mechanisms in different cortical areas, and their interactions. Here we study patterns of surround modulation in primary visual cortex (V1) and middle temporal complex (hMT+) utilizing a well-studied effect in motion perception, where human observers' ability to discriminate the drift direction of a grating improves as its size gets bigger if the grating has a low contrast, and deteriorates if it has a high contrast. We first replicated the findings in the literature with a behavioral experiment using small and large (1.67 and 8.05 degrees of visual angle) drifting gratings with either low (2%) or high (99%) contrast presented at the periphery. Next, using functional MRI, we found that in V1 with increasing size cortical responses increased at both contrast levels. Whereas in hMT+ with increasing size cortical responses remained unchanged or decreased at high contrast, and increased at low contrast, reflecting the perceptual effect. We also show that the divisive normalization model successfully predicts these activity patterns, and establishes a link between the behavioral results and hMT+ activity. We conclude that surround modulation patterns in V1 and hMT+ are different, and that the size-contrast interaction in motion perception is likely to originate in hMT+.

1. Introduction

Visual neurons respond to stimuli only within their classical receptive fields (RF) when these stimuli are presented in isolation. If, however, the RF and its surround are stimulated together, the response patterns of the neurons alter. This kind of surround modulation is found in many levels of the visual hierarchy (Angelucci et al., 2017). Yet many questions about the mechanism remain open. Most importantly, even though surround modulation is heavily studied in primary visual cortex (V1), it is not clear whether the basic principles of the mechanism remains the same for a variety of stimuli in other visual areas. Here, to tackle this question we used a well-known perceptual effect in motion perception and investigated surround modulation in V1 and human middle temporal complex (hMT+).

In the aforementioned perceptual effect, as the size of a drifting grating increases, discriminating its motion direction becomes harder if it has high contrast, but easier if it has low contrast (Tadin et al., 2003). This perceptual effect has been attributed to the surround modulation of neuronal populations in hMT+, which is one of the central cortical areas in motion processing ('MT-hypothesis', Tadin et al., 2003). According to the MT-hypothesis, discriminating motion direction of a high-contrast grating becomes harder owing to the suppressive effects of surround stimulation (i.e. surround suppression). For a low contrast grating, on the other hand, motion direction discrimination becomes easier as its size gets larger owing to facilitative effects of surround stimulation (i.e. surround facilitation). The MT-hypothesis has been later supported by functional magnetic resonance imaging (fMRI) findings (Turkozer et al., 2016; Schallmo et al., 2018). Furthermore, disrupting hMT+ activity with application of TMS resulted in decreased surround suppression for high-contrast stimuli (Tadin et al., 2011). These results all support the hypothesis that size-contrast interaction in motion perception could originate in hMT+ owing to surround modulation mechanisms.

* Corresponding author.
E-mail address: zahide_pamir@meei.harvard.edu (Z. Pamir).
[1] Equal contribution, alphabetical order.
[2] Present address: Schepens Eye Research Institute of Massachusetts Eye and Ear, Department of Ophthalmology, Harvard Medical School, Boston, MA, USA.

https://doi.org/10.1016/j.neuroimage.2020.117084
Received 7 October 2019; Received in revised form 13 June 2020; Accepted 21 June 2020
Available online 3 July 2020

Previous studies, however, were not able to address the question of the role of other cortical areas in the observed perceptual effect. For example, neuronal correlates of spatial suppression and facilitation within the hMT+ might be inherited from earlier visual areas, most notably from V1. This possibility has not been systematically analyzed in humans yet. One major cause of this was related to methodological limitations: Previous studies investigating the size-contrast interaction in motion perception used foveally presented stimuli, which activate neurons in the so-called foveal confluence, where borders of V1, V2, and V3 are difficult to draw using fMRI (e.g. Turkozer et al., 2016; Schallmo et al., 2018). Thus, in those studies it was not possible to confidently investigate the activity of V1 along with hMT+. In the current study we overcome this limitation by presenting the stimuli at the periphery, where it becomes straightforward to identify regions of interest in different early visual areas. In this way we were able to investigate the roles of both hMT+ and V1 in the perceptual effect.

Another open question is about the exact neuronal mechanism underlying the perceptual effect. In a recent study, Schallmo et al. (2018) performed numerical simulations of neuronal activity in response to small and large drifting grating patterns at various contrast levels. In their simulations they used the divisive normalization model (Heeger, 1992; Carandini and Heeger, 2012; Reynolds and Heeger, 2009) with parameters based on monkey MT+ literature. Their results showed that the behavioral effect could parsimoniously be explained by the divisive normalization model, and there is no need to utilize two separate mechanisms, namely one suppressive mechanism at high contrast and another facilitative mechanism at low contrast (Schallmo et al., 2018). Whether the same model can predict the responses to stimuli presented at the periphery, however, remains to be tested.

Here we first conducted a behavioral experiment to ensure that the perceptual effect persists when the stimulus is presented at the periphery. After ensuring that the perceptual effect is present, using fMRI we investigated the neuronal responses within hMT+ and V1 in response to drifting gratings in varying contrast and size levels. Finally we simulated neuronal and cortical responses in hMT+ and V1 using the divisive normalization model.

2. Experiment 1: Behavioral Experiment

2.1. Methods

2.1.1. Participants

Eleven participants, including the authors ZP and GE, participated in the experiment (seven female; age range: 19–28). All participants reported normal or corrected-to-normal vision, and had no history of neurological or visual disorders. Prior to the experimental sessions participants gave their written informed consents. Experimental protocols and procedures were approved by the Human Ethics Committee of Bilkent University.

2.1. Stimuli, experimental procedures, and analyses

Visual stimuli were presented on a CRT monitor (HP P1230, 22 inch, 1600 × 1200 resolution, 120 Hz). Participants were seated 75 cm from the monitor, and their heads were stabilized using a chin rest. Responses were collected via a standard computer keyboard. A gray-scale look-up table, prepared after direct measurements (SpectroCAL, Cambridge Research Systems Ltd., UK), was used to ensure the presentation of correct luminance values. The experimental software was prepared by us using the Java programming platform.

Stimuli were horizontally oriented drifting sine wave gratings (spatial frequency: 1 cycle per degree) weighted by two-dimensional isotropic Gaussian envelopes. Two size- and contrast-matched gratings were simultaneously and briefly presented on a mid-gray background (40.45 cd/m^2) at ± 9.06 degrees of horizontal eccentricity (the visual angle between the central fixation and the center of the gratings). Each grating drifted within the Gaussian envelope (starting phase randomized) at a rate of 4°/s either upward or downward. Participants reported whether or not the gratings drifted in the same direction, while maintaining fixation at the central fixation mark. After responding, participants received an auditory feedback (auditory tone of 200 ms duration, 300 Hz for correct and 3800 Hz for incorrect answers). Two size levels (small: 1.67°, large: 8.05° visual angle in diameter) and two contrast levels (2% and 99% Michelson contrast) were tested (4 experimental conditions in total). Based on the average excitatory center and inhibitory surround extent of a typical MT and V1 neuron's receptive field, the small stimulus size was selected to be small enough to stay within the excitatory center and the large stimulus size was selected to be large enough to evoke response from the inhibitory surround of the receptive field (Albright and Desimone, 1987; Angelucci and Shushruth, 2013; Amano et al., 2009; Sceniak et al., 1999). Each condition was blocked in a separate session of 160 trials, and the sessions were randomly ordered for each participant. Participants completed a short practice session before beginning an experimental session. Based on their performance in the practice session, initial presentation duration parameter for the experimental sessions were selected per participant. For the ensuing trials, presentation duration was manipulated adaptively with a two interleaved 3-up 1-down staircase procedure. One staircase started from a relatively short duration, the other started from a longer duration. Each staircase was terminated after 80 trials.

Psychometric functions were fit to the data using the Palamedes toolbox (Kingdom and Prins, 2010) in Octave (http://www.octave.org) for each observer and condition. Duration thresholds (79% success rate) and standard errors were estimated. Repeated-measures analysis of variances (ANOVA) with two factors (size and contrast) was performed to compare the thresholds at group level using SPSS Version 19 (SPSS Inc., Chicago, IL). Additionally, to facilitate drawing links between the behavioral results and fMRI findings, we calculated "sensitivity" values, defined as 1/threshold. Next using the sensitivities for large and small gratings, S_L and S_S respectively, we computed a size index (*SI*) defined as $SI = S_L - S_S$. A positive *SI* means increased sensitivity with increasing size (spatial facilitation), a negative *SI* means decreased sensitivity with increasing size (spatial suppression). We compared the *SI* values to "0" by applying one-sample two-tailed Student's *t*-test in SPSS. Also, *SI* values for low and high contrast conditions were compared using two-tailed paired-samples *t*-test.

2.2. Results

We measured duration thresholds for accurately judging the drift direction of gratings presented at the periphery at two size (1.67° and 8.05°) and contrast levels (2% and 99%). Results are shown in Fig. 1. Analyses showed that main effect of contrast was statistically significant ($F(1,10) = 12.16$, $p < 0.01$) and main effect of size was close to significance ($F(1,10) = 4.49$, $p = 0.06$). Also, the interaction between contrast and size was statistically significant ($F(1,10) = 33.96$, $p < 0.001$). Bonferroni corrected pairwise comparisons showed that for the high-contrast gratings thresholds increased with size ($t(10) = -4.1$; $p < 0.01$; small stimuli: M = 39.83, SEM = 2.24; large stimuli: M = 99.8, SEM = 13.02) whereas for the low-contrast gratings the thresholds decreased with size ($t(10) = 6.03$; $p < 0.001$; small stimuli: M = 107.9, SEM = 6.23; large stimuli: M = 81.18, SEM = 6.22). Consistent with the pairwise comparisons applied to the raw threshold values, one-sample two-tailed Student's *t*-tests showed that the size index (*SI*, see methods) was significantly lower than zero for the high-contrast gratings ($t(10) = -5.53$; $p < 0.001$; M = -0.014, SEM = 0.002) whereas it was significantly higher than zero for the low-contrast gratings ($t(10) = 5.56$; $p < 0.001$; M = 0.003, SEM = 0.0006). Also, two-tailed paired-samples Student's *t*-tests showed that SI was significantly higher for low-contrast stimuli compared to that for high-contrast stimuli ($t(10) = 6.97$; $p < 0.001$). These results successfully replicate the size–contrast interaction in motion perception when stimuli is presented at the periphery.

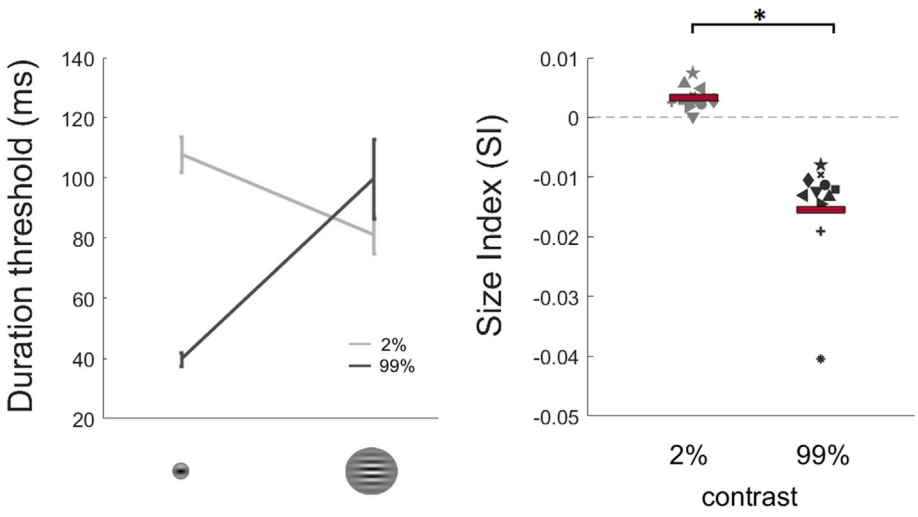

Fig. 1. Left plot shows group mean ($N = 11$) of duration thresholds. For low-contrast stimuli, discrimination threshold decreases as size gets bigger. On the contrary, for high-contrast stimuli, discrimination threshold increases as size gets bigger. Right plot shows individual participants, and the group mean (red bars) size indices (*SIs*) for 2% and 99% contrast levels. *SI* is defined as the difference in sensitivity (1/threshold) between large and small gratings. For low-contrast stimuli, *SI* is positive which indicates that sensitivity increases as size gets bigger, i.e. spatial facilitation. On the contrary, for high-contrast stimuli, sensitivity decreases as size gets bigger, i.e. spatial suppression. These results replicate the size–contrast interaction in motion perception when stimuli is presented at the periphery. Error bars represent ± SEM. ($*p < 0.001$).

3. Experiment 2: fMRI Experiment

3.1. Materials and methods

3.1.1. Participants

Six volunteers (age range: 23–26; mean age: 25; three male) participated in the experiment, three of whom also participated in the behavioral experiment. All participants had normal or corrected-to-normal vision and had no history of neurological or visual disorders. Participants gave their written informed consents prior to the fMRI sessions. Experimental protocols and procedures were approved by the Bilkent University Human Ethics Committee.

3.1.2. Data acquisition & experimental setup

MR images were collected in the National Magnetic Resonance Research Center (UMRAM), Bilkent University on a 3 Tesla MR scanner (Magnetom Trio, Siemens AG, Erlangen, Germany) with a 32-channel array head coil. MR sessions started with a structural run followed by three region of interest (ROI) localizer and four experimental functional runs, totaling approximately 1 h in duration. One localizer run was used to identify the hMT+ region, the other two were for localizing the subregions of hMT+ and V1 that process the input from the visual field that correspond to the position and size of the small gratings (see below 3.1.3 "Visual Stimuli & Experimental Design"). Structural data were acquired using a T1-weighted 3-D anatomical sequence (TR: 2600 ms, spatial resolution: 1 mm^3 isotropic, number of slices: 176). Functional images were acquired with a T2*-weighted gradient-recalled echo-planar imaging (EPI) sequence (TR: 2000 ms; TE: 35 ms; spatial resolution: 3x3x3 mm^3; number of slices: 30; slice orientation: parallel to calcarine sulcus). Visual stimuli were presented on an MR-safe LCD Monitor (TELEMED PMEco, Istanbul, Turkey; 32 inch; resolution: 1920x1080; vertical refresh: 60 Hz). The monitor was placed near the rear end of the scanner bore, and viewed by the participants from a distance of 165 cm via a mirror mounted on the head coil. The stimuli were generated and presented using Python and the Psychopy package (Peirce, 2009).

3.1.3. Visual Stimuli & Experimental Design

Visual stimuli were drifting gratings as in the behavioral experiment. Two size (small: 1.67°, large: 8.05°) and two contrast levels (2% and 99%) were tested. Size (diameter) was defined as six times the standard deviation of the Gaussian envelope in the fMRI experiment. FMRI experimental code was written in Python using the built-in methods of the Psychopy package, whereas the behavioral experiment was written using custom Java modules developed by us. Therefore, the formulation and implementation was slightly different in the behavioral experiment. Nevertheless, the stimuli were ensured to have same sizes in both experiments. Due to the limits of the visual display system, gratings were presented at ± 8.02 degrees of horizontal eccentricity (was 9.06° in the behavioral experiment), and drifted with a rate of 6°/s (was 4°/s in the behavioral experiment) either upward or downward for the duration of 12 s. Both gratings drifted in the same direction simultaneously, and alternated direction every 2 s to avoid motion adaptation.

A functional run was composed of "active" and "control" blocks, each lasting for 12 s. In the active blocks, drifting gratings and a central fixation mark were presented, whilst in the control blocks, only the fixation mark remained visible. In alternating active blocks, small and large drifting gratings were shown, each repeated for 6 times in a run. Contrast level was kept constant within a run. Two experimental runs were conducted for each contrast level in a session. The runs started with an initial blank period of 24 s to allow hemodynamic response to reach a steady state. The total duration of a functional run was around 5 min. Fig. 2 shows the schematic representation of an experimental run.

Both to ensure fixation and to control for spatial attention,

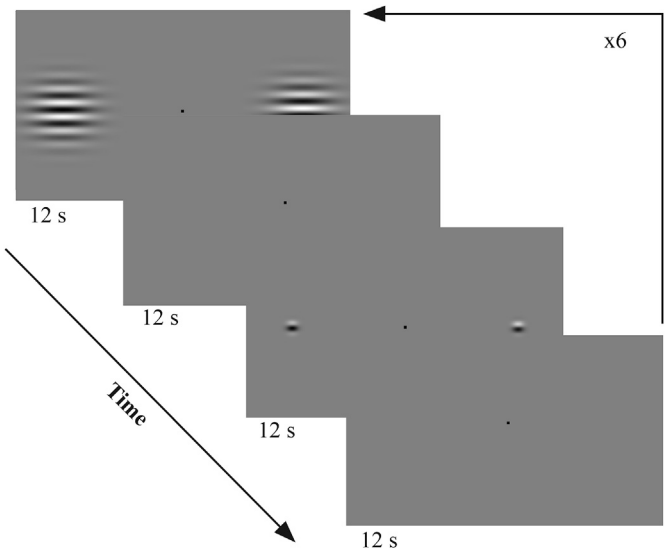

Fig. 2. Schematic representation of the visual paradigm of a single cycle in the fMRI experiment. This cycle is repeated for 6 times within a run. Large (8.05°) and small (1.67°) drifting gratings were presented in alternating active blocks. The contrast was kept constant in a run (2% or 99%), and two runs were conducted for each contrast. Participants were required to keep fixation at the central mark, and perform a demanding fixation task.

participants were asked to perform a demanding fixation task throughout an entire functional run (all participants achieved a mean accuracy rate of over 90%, which was the predetermined threshold to discard the participant's data). The color of the fixation mark (0.3-degree solid square) changed randomly from its original color (gray) to either red or yellow for the duration of 50 ms at the randomly designated interval between 250 and 1500 ms. The participants' task was to report the changes in the color of the fixation mark by pressing the designated button on an MR-safe response button-box (Fiber Optic Response Devices Package 904, Current Designs).

3.1.4. hMT+ and V1 identification

We identified the hMT+ complex in a separate run using the established methods in literature (Huk et al., 2002; Dukelow et al., 2001; Smith et al., 2006). Specifically, we presented the participants fields of moving dots while acquiring functional MR images. The dot fields were comprised of 100 dots on a black background within an 8-degree diameter circular aperture. The centers of the fields were 8.02° to the left and right of the fixation point. The dots moved in three different trajectories: radial (expanding - contracting), cardinal (left - right; up - down), and angular (clockwise - counterclockwise). Motion direction changed every 2 s to prevent adaptation. BOLD responses were collected for three types of configurations, each presented for 12 s: right field dynamic (left static), left field dynamic (right static), and both fields static. This cycle of the presentation was repeated eight times in a run. We used general linear model (GLM) to contrast the BOLD responses during dynamic and static presentations. Voxels that respond more strongly to contralateral dynamic compared to static stimuli at the ascending tip of the inferior temporal sulcus were identified as hMT+.

Using flickering (5 Hz) checkerboard stimuli in an independent localizer run, we identified V1 voxels that respond more strongly to the locations of the small-sized gratings. The checkerboard stimuli had the same sizes and locations as the gratings used in the experimental run. The protocol of this functional localizer run was the same as the experimental run: 12 s small and large sized blocks were interspersed with 12 s blank trials. Large and small sized checkerboard stimuli were used in the run, however, only small-sized ones were used in the identification of the V1 mask. Several clusters of active voxels were found using a liberal statistical threshold, and the voxels that fell in or around the calcarine sulcus in this step were identified as V1 voxels for further analyses.

3.1.5. ROI localization within hMT+ and V1

Functional localizer. In order to identify subregions within hMT+ and V1 that are selectively more responsive to the visual field that correspond to the locations of the small gratings, we performed an independent localizer run (see Fig. 3). This localizer run was composed of 12 s active blocks separated by 12 s rest blocks. In alternative active blocks, we presented small and large gratings. Sizes and locations of the gratings were the same as in the main experiment. Their contrast, however, was 60%, because we wanted to use a mid-level contrast between the two extreme contrasts used in the experiment in order not to bias the choice of voxels to one contrast or the other. Throughout the entire run participants were required to maintain central fixation and perform a demanding fixation task as described before. Subsequent analyses using this localizer run are described below.

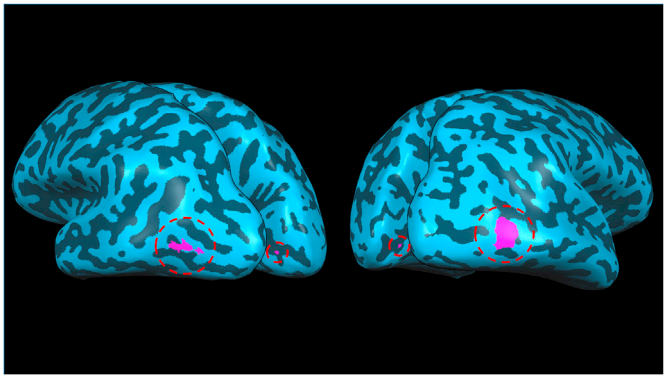

Fig. 3. Location of V1 and hMT+ ROIs on the inflated hemispheres for a representative participant. V1 and hMT+ ROIs are marked with small and large dashed circles respectively. These ROIs were identified using an independent localizer run with 60% gratings.

ROI within hMT+. We identified the regions of interest in hMT+ in three steps. In the first step (Step 1), we identified hMT+ using a functional localizer (i.e. moving vs. stationary dots as explained above). In the following steps the goal was to identify the voxels within hMT+ that contain neurons whose receptive field centers were in the visual space occupied by the small gratings. To achieve this goal, we first performed a GLM contrast between small-sized drifting gratings and the rest block. This gave us the voxels that respond more strongly during the presentation of the small-sized gratings compared to rest (Step 2). Some of these voxels, however, could have their center of population receptive fields outside of the locations that correspond to the small gratings. To exclude those voxels we performed another step (Step 3). In this step we compared the BOLD responses of the voxels to the small gratings and large gratings. We excluded the voxels that responded more strongly (simple numerical comparison) to the large-sized gratings from those we obtained in Step 2. This finalized the ROI selection. To further test the effect of voxel selection, we repeated the analyses using only the most significant 50 voxels in Step 3, 14 voxels that were approximately located at the geometric center of the ROI identified in Step 3, and all the voxels obtained in Step 3 (see Supplement for the false discovery rate (FDR) thresholds and number of voxels in each ROI for each participant). All analysis methods led to statistically identical results (See Supplement).

To further investigate the responses we have defined a more selective alternative ROI in hMT+. Here, the first two steps were the same as described above. This time, however, in the last step, we used one of the high-contrast (99%) runs to localize the ROI, and analyzed the rest of the runs within that ROI. More specifically, based on the numerical comparison, we identified voxels that showed the strongest preference for small compared to large stimuli in each hemisphere for each participant in one of the high-contrast runs. The number of such voxels ranged from 5 to 45 (see Supplement for the number of voxels in each ROI for each participant). Next within these ROIs we computed the BOLD responses in the remaining three runs (the other high-contrast run and the two low contrast runs). We repeated the same procedure using the other high-contrast run as the localizer, and computing the BOLD responses in the remaining three runs. It was not possible to identify voxels that respond more strongly to small stimuli compared to large stimuli in the left hemisphere of one participant in one of the high contrast runs. For that specific participant and hemisphere we picked the voxels whose responses to large stimuli were closest to those of small stimuli.

ROI within V1. We identified the V1 ROIs with a very similar approach by using three steps. We first identified the V1 voxels that respond more strongly to the locations of the small-sized gratings using flickering checkerboard stimuli (Step 1, as explained above). In Step 2, using the functional localizer with gratings, we identified the voxels that responded more strongly to small-sized drifting gratings compared to the rest condition. Finally, in Step 3, we excluded the voxels that responded more strongly (simple numerical comparison) to the large-sized gratings compared to small-sized gratings. This finalized our V1 ROI identification. As we did for the hMT+ voxels, we analyzed the experimental data using different ROI selection methods and found statistically identical results (See Supplement).

We attempted to perform a similar more selective alternative ROI identification as we did for hMT+. But this was not possible. Using the 99% contrast gratings, we could not reliably identify the voxels that respond more strongly to the small gratings compared to the large gratings across all participants in V1.

3.1.6. Analyses

Anatomical and functional data were preprocessed and analyzed using the BrainVoyager QX software (Brain Innovation, The Netherlands). Preprocessing steps for the functional images included head motion correction, high-pass temporal filtering and slice scan time correction. T1-weighted structural images were transformed into the AC-PC plane, and aligned with the functional images. For each brain, the border between white matter and gray matter was drawn, and an inflated three-dimensional model of the cortex was generated. Functional maps were projected onto the inflated cortex to aid the visualization of subsequent analyses. hMT+, and subregions (ROIs) within hMT+ and V1 were identified with GLM as described before using BrainVoyager (see Fig. 3).

Statistical analyses were performed on BOLD responses computed using the beta weights calculated with GLM within the ROIs. To further quantify the changes in BOLD response evoked by an increase in stimulus size, and to draw links with behavioral results, we calculated an fMRI size index (*SI*) defined as $SI = B_L - B_S$, where B_L and B_S are the BOLD responses for large and small gratings, respectively. A positive *SI* denotes an increased BOLD response with increase in size (surround facilitation), and a negative *SI* denotes decreased BOLD response (surround suppression). To compare the BOLD responses at the group level, a 2 × 2 repeated-measures ANOVA was conducted with contrast (low and high) and size of the stimuli (small and large) as factors. We applied one-sample two-tailed Student's *t*-test to compare *SIs* to "0" at each contrast level. We also performed paired samples *t*-test to compare the *SIs* to each other (low versus high contrast). Statistical analyses were conducted using JASP Version 0.8.5 (JASP Team, 2018).

3.1.7. Normalization model

We used the divisive normalization model to simulate neuronal and cortical responses to the experimental stimuli (Heeger, 1992; Reynolds and Heeger, 2009; Carandini and Heeger, 2012). The model was recently shown to successfully predict the center-surround interaction in humans under experimental conditions similar to ours (Schallmo et al., 2018). In the model, a unit at position (x,θ) in a 2-dimensional position-orientation space responds to a stimulus with contrast *c* by

$$R(x,\theta,c) = \frac{E(x,\theta,c)}{S(x,\theta,c)+\sigma} \quad (1)$$

where *E* and *S* are the excitatory and suppressive drives respectively, and σ, semi-saturation constant, is a small positive number. *E* is computed as a weighted sum of excitatory input across a summation field

$$E(x,\theta,c) = e(x_e,\theta_e,c)*N(x,\theta,c), \quad (2)$$

where *e* is the excitatory summation kernel (e.g. a Gaussian), * denotes convolution, and *N* is an abstracted neuronal image in response to the visual stimulus (response of a Gaussian filter centered on x, theta, scaled by contrast, c). The suppressive drive is computed as another weighted sum

$$S(x,\theta,c) = s(x_s,\theta_s,c)*E(x,\theta,c), \quad (3)$$

where *s* is the suppression kernel.

To compute the neuronal and cortical responses we followed two approaches. In the first approach, we sought to model the cortical responses obtained using fMRI. Because the unit of activation in the fMRI data is a voxel containing many neurons, we computed the sum of responses of units within a neighborhood in the (x,θ) space centered on the stimulus

$$R(c) = \sum_{x\in\mathcal{N}(s)}\sum_{\theta} R(x,\theta,c) \quad (4)$$

where $\mathcal{N}(s)$ means the neighborhood of stimulus position. In our simulation we used ±5 neighborhood of the stimulus center (x). We call these "Population Responses".

In the second approach, we identified the unit with the maximum response, and used that value as the system's overall response at that contrast

$$R(c) = \max(R(x,\theta,c)). \quad (5)$$

Note that this "winner-take-all" approach was adapted in Schallmo et al. (2018) study. We call these "Single Unit Responses".

Table 1 reports the parameters used in simulations based on the literature (Albright and Desimone, 1987; Angelucci and Shushruth, 2013; Amano et al., 2009; Sceniak et al., 1999). Simulations were done on Octave platform Version 4.2.2 (www.octave.org). The code was an implementation of the model introduced in Reynolds and Heeger (2009) (also see Schallmo et al., 2018). We simulated responses for only one hemifield assuming symmetry.

3.2. Results

In this experiment, we recorded and analyzed BOLD responses in hMT+ and V1 while the observers viewed peripherally presented drifting gratings. We compared the magnitudes of BOLD responses between small and large gratings at two contrast levels within predefined ROIs that correspond to the location and size of small stimuli (i.e. "center"). Because our goal here is to measure the modulatory effect of surround stimulation on the responses of the neurons whose classical RF centers are inside the visual space that correspond to the small grating, BOLD response differences evoked by presenting the large and small-sized stimuli would highlight the suppressive or facilitative influence of the surround on the center.

3.2.1. hMT+

We computed the BOLD responses within independently identified ROIs as described above. In addition to those "original" ROIs, in hMT+ we identified a more selective group of voxels, as well. For this "alternative" ROI, we identified the voxels that respond to the region occupied by the small stimuli and at the same time respond more strongly to small stimuli compared to large stimuli at high contrast (Methods).

Fig. 4 (left column) shows the results from hMT+ in the original ROI. Increasing the size of the stimuli resulted in increased BOLD response, when stimuli had low contrast. Conversely, increasing size of the stimuli resulted in no change in BOLD response when stimuli had high contrast. To test whether stimulus contrast and size affect the magnitude of BOLD response significantly, we applied a 2 × 2 repeated-measures ANOVA for the contrast (2% and 99%) and size (small and large) as factors. Results revealed that there was no main effect of contrast ($F(1,5) = 2.886$, $p = 0.151$), but there was a main effect of size ($F(1,5) = 18.299$, $p = 0.008$), as well as an interaction between size and contrast ($F(1,5) = 12.433$, $p = 0.017$).

To further investigate the patterns of results, we computed size indices (*SIs*), defined as the difference between the BOLD responses to large and small gratings (see Methods). Fig. 4 shows individual *SI* values

Table 1
Normalization model parameters for MT+ and V1.

Symbol	Description	Value	
		MT+	V1
c	Stimulus contrast	0.02, 0.99	0.02, 0.99
x_e	Excitatory spatial summation kernel width	5	2
x_s	Suppressive spatial summation kernel width	40	8
θ_e	Excitatory orientation summation kernel width	20	5
θ_s	Suppressive orientation summation kernel width	50	8
σ	Semi-saturation constant	0.0002	0.0002
$\mathcal{N}(s)$	Neighborhood of stimulus position (in x dimension) in "Population Responses"	±5	±5

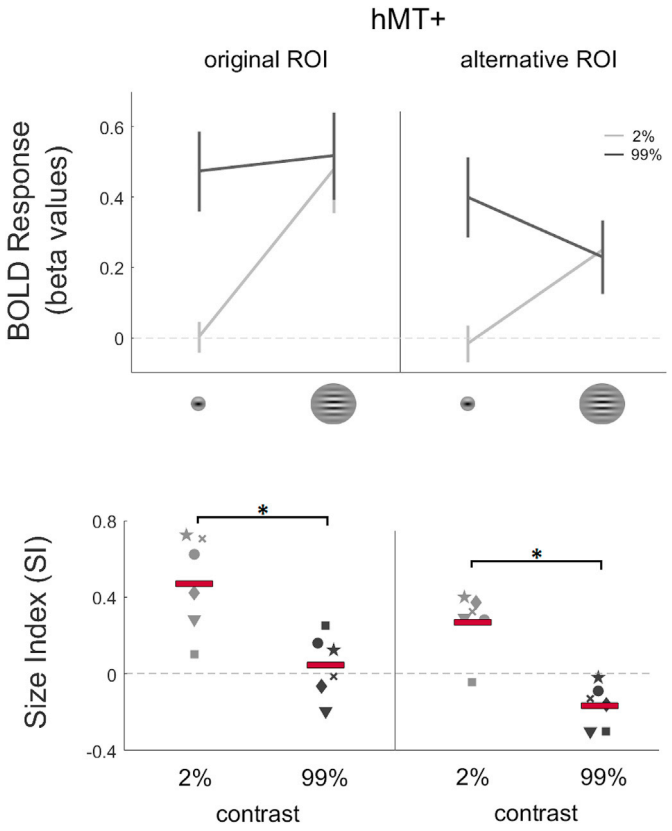

Fig. 4. hMT+ results. Upper row, group mean ($N = 6$) of BOLD responses. The original ROI is identified using an independent localizer run, alternative ROI is identified more selectively using one of the high contrast runs. In the latter case the experimental data from the remaining three runs are analyzed. BOLD responses to small and large stimuli with high and low contrast were extracted from these ROIs. Average responses from the ROIs were computed for each subject, then the group mean was calculated. Lower row, fMRI size indices (*SI*) in hMT+ for individual participants, and the group mean (red bars). *SI* is defined as the difference in BOLD response between large and small stimuli. A positive *SI* indicates surround facilitation, a negative one surround suppression. The pattern of *SI*s is consistent with the behavioral results (compare with Fig. 1, right plot). (Error bars represent ±SEM; *$p < 0.05$).

for all participants, as well as the mean *SI*. We found that *SI* was significantly different (greater) than zero at low contrast (M_{SI}= 0.477, SEM = 0.103; one-sample *t*-test, $t(5) = 4.66$, $p = 0.003$). On the other hand, the *SI* at high contrast was not significantly different than zero (M_{SI}= 0.044, SEM = 0.067; one-sample *t*-test, $t(5) = 0.66$, $p = 0.269$). Furthermore, based on the results in literature (Turkozer et al., 2016; Schallmo et al., 2018), we expected a larger *SI* for low contrast compared to high contrast. Indeed, paired sample *t*-test results revealed that the *SI*s were statistically significantly different, the *SI* for low-contrast being greater than that for the high-contrast ($t(5) = 3.53$, $p = 0.017$).

Fig. 4, right column shows the results from the alternative ROIs. Within these ROIs, we found surround facilitation at low contrast and surround suppression at high contrast. Consequently, *SI* was positive for low contrast and negative for high contrast. Furthermore, *SI* was greater for low contrast than high contrast.

To statistically test the effects, we applied a 2 × 2 repeated-measures ANOVA for the contrast (2% and 99%) and size (small and large) as factors. Results of the repeated-measures ANOVA revealed no main effect of contrast ($F(1,5) = 2.190$, $p = 0.199$), no main effect of size ($F(1,5) = 0.930$, $p = 0.379$), but a statistically significant interaction between size and contrast ($F(1,5) = 80.262$, $p < 0.001$). Paired samples *t*-test revealed that the mean BOLD response evoked by the large-sized stimuli was significantly greater than the mean BOLD response evoked by the small-sized stimuli at low contrast ($M_{large} = 0.253$, SEM = 0.058; $M_{small} = -0.017$, SEM = 0.049; $t(5) = 4.09$, $p = 0.009$). At high contrast, the mean BOLD response evoked by the large-sized stimuli was significantly less than the mean BOLD response evoked by the small-sized stimuli ($M_{large} = 0.231$, SEM = 0.108; $M_{small} = 0.402$, SEM = 0.116; $t(5) = 3.71$, $p = 0.014$). One-sample *t*-test results showed that group mean of *SI* was significantly different (greater) than zero at low contrast (M_{SI}= 0.270, SEM = 0.066; one-sample *t*-test, $t(5) = 4.09$, $p = 0.009$), and significantly different (lower) than zero at high contrast ($M_{SI} = -0.171$, SEM = 0.046; one-sample *t*-test, $t(5) = -3.17$, $p = 0.014$). In line with this, paired sample *t*-test results revealed that the group mean of *SI* for low-contrast was greater than for high-contrast ($t(5) = 8.98$, $p < 0.001$).

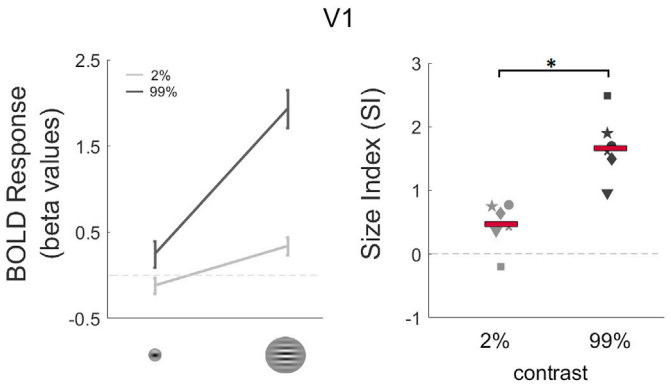

Fig. 5. V1 results. Left plot, group mean ($N = 6$) of BOLD responses. Right plot, fMRI size indices (*SI*) for individual participants, and the group mean (red bars). The pattern is inconsistent with the perceptual effect (compare to behavioral results in Fig. 1) and is different than the pattern observed in hMT+ (Fig. 4). (Error bars represent ± SEM; *$p < 0.05$).

3.2.2. V1

We next analyzed how the size and contrast of stimuli affect BOLD responses within the V1 ROI. Fig. 5 shows the responses for each condition. Results showed that BOLD responses increased significantly with size both at high and low contrast conditions. Critically, this increase was greater when the stimuli had high contrast compared to low contrast. This pattern was inconsistent with the perceptual effect, and was different than the pattern observed in hMT+. We applied two-way repeated-measures ANOVA with the contrast (low and high) and size (small and large) as factors to investigate the role of contrast and size on the BOLD response. ANOVA revealed a main effect of contrast, ($F(1,5) = 19.93$, $p = 0.007$), and size ($F(1,5) = 129.98$, $p < 0.001$), as well as a significant interaction between size and contrast ($F(1,5) = 16.63$, $p = 0.010$).

As we did for the hMT+ data, here too we performed further analyses on *SI*s. Fig. 5 (right plot) shows *SI*s plotted for individual participants, as well as the group mean. At low contrast, group mean of *SI* was significantly greater than zero ($M_{SI} = 0.458$, SEM = 0.148; one-sample *t*-test, $t(5) = 3.10$, $p = 0.013$). Average *SI* value was positive at high contrast, as well ($M_{SI} = 1.689$, SEM = 0.204; one-sample *t*-test, $t(5) = 8.290$, $p < 0.001$). Furthermore, we performed paired sample *t*-test, and found that the *SI* value for low contrast was significantly lower than the *SI* value for high contrast ($t(5) = -3.36$, $p = 0.028$).

We tried to identify a more selective alternative ROI within V1 as we did in hMT+. Applying the same procedures, however, did not allow us reliably identify alternative ROIs in V1 for every participant. Therefore, we did not pursue analyzing the experimental data in alternative ROIs in V1.

3.3. Comparing behavioral and fMRI results

To draw a link between the behavioral and fMRI results, we first as-

sume that behavioral sensitivity (1/ duration threshold) can be approximated by a monotonically increasing function of the amount of neuronal responses. Further, we assume a linear relation between neuronal activity and the BOLD fMRI response (see e.g. Boynton, Demb, Glover, 458 & Heeger, 1999). Thus, if an area is involved in the processes related to the perceptual effect, we expect an increase in fMRI BOLD response in that area as the behavioral sensitivity gets better. Consequently we expect the pattern of fMRI *SIs* reflect the behavioral ones. Comparing the duration thresholds (Fig. 1, left plot), and BOLD responses (Fig. 4), we see that the hMT+ activity captures the behavioral results for low contrast stimulus. For high contrast stimulus, the pattern in the alternative ROI is consistent with behavior (Fig. 4, right column). The pattern obtained from the less selective original ROI, however, seems to be in slight disagreement with the behavioral results (Fig. 4, left column) (see Discussion for possible reasons for this). The V1 activity, on the other hand, is completely inconsistent with the behavioral results. This pattern becomes more clear when the size indices are compared (Fig. 1 right plot, and Fig. 5 right plot). Overall the response patterns in hMT+, but not in V1, agree with the behavioral results.

3.4. Normalization model

In a recent publication Schallmo et al. (2018) showed that both surround facilitation and suppression can be explained using a single divisive normalization model (Heeger, 1992; Carandini and Heeger, 2012). Briefly, in the divisive normalization model response of a population of neurons is determined by the ratio of excitatory and inhibitory drives it receives (see Methods). In their experiments Schallmo et al. (2018) used gratings with different sizes and contrasts, as we did here. Their stimuli, however, were presented foveally. Here, we sought to find whether such a simple model could also explain our findings in V1 and hMT+ when the stimuli are presented peripherally. To test whether the divisive normalization model can also explain our results, we used an approach similar to that used by Schallmo et al. (2018). We determined the summation field sizes for the excitatory and inhibitory drives based on the reported RF properties of neurons in MT+ and V1 in the literature (Albright and Desimone, 1987; Angelucci and Shushruth, 2013; Amano et al., 2009; Sceniak et al., 1999) (see Table 1 in Methods for the parameter values). To compare model predictions to BOLD responses, we simulated the activity of a population of units, representing a virtual voxel centered directly on the stimulus. Fig. 6 shows the results. These results are in good agreement with our empirical data. The model predicts suppression at high contrast in hMT+ (using monkey MT+ parameters), and facilitation at low contrast. Moreover, the model predicts facilitation at both low and high contrast in V1 (using monkey V1 parameters), again consistent with our findings.

Given these results, one may wonder whether the model would predict a different pattern at the single unit level. To investigate this we computed and compared the activity of a single maximally responsive unit under each condition. These results are shown in Fig. 7. Whereas the MT+ model prediction pattern does not change, i.e. we observe suppression at high contrast, and facilitation at low contrast, the V1 model predictions drastically change. Now in V1 at both contrast levels the model predicts suppression. These results show that the model does indeed predict surround suppression in V1 at the single unit level, but this effect is not captured at the population level.

4. Discussion

We demonstrated that the pattern of activity in hMT+ complex, but not in V1, agrees with size-contrast interaction in motion perception. First, in a behavioral experiment we measured the temporal thresholds for successfully detecting the direction of motion of drifting gratings presented at the periphery. We found that the thresholds decreased with size (i.e. increased sensitivity, spatial facilitation) if the target has low contrast (2%). Conversely, we found that the thresholds increased with

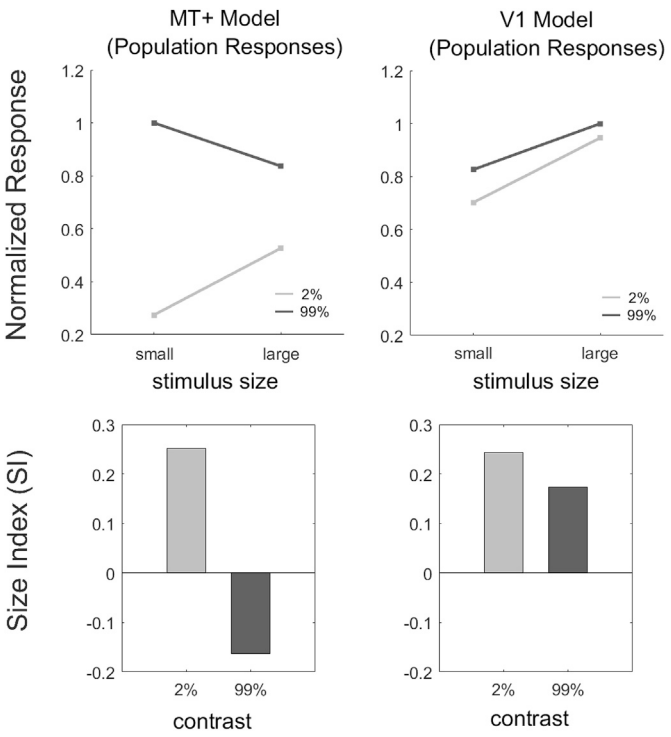

Fig. 6. Divisive normalization model simulations based on the activity of a population of units in a virtual voxel centered on the stimuli. For V1 and MT+ we used receptive field parameters based on monkey literature. MT+ model predictions agree both with our behavioral findings and the pattern of BOLD responses we observed in hMT+. V1 model predicts the BOLD responses we observed in V1. But this pattern does not agree with the behavioral effect.

size (i.e. decreased sensitivity, spatial suppression) if the target has high contrast (99%). These results were in good agreement with literature (e.g., Tadin et al., 2003). Next, we recorded fMRI BOLD responses while participants viewed high- and low-contrast, small and large drifting gratings presented at the periphery. In hMT+ we found that BOLD responses significantly increased with size for the low contrast gratings (surround facilitation), and remained unchanged or decreased (surround suppression) for the high contrast gratings. In V1, however, BOLD responses increased for both high and low contrast gratings. These results show that hMT+ activity reflects the behavioral effect, but V1 activity does not. Furthermore, our numerical simulations show that BOLD responses in both hMT+ and V1 are predicted by the divisive normalization model.

We identified the regions of interest (ROIs) in hMT+ using two methods. In one of them, we used the results of an independent localizer run, where 60% gratings were presented. In a second approach, we identified the ROIs more selectively using the data from one of the 99%-contrast runs. In the latter approach, we analyzed the data only in the remaining three experimental runs. Using the first approach we found that as size increases BOLD responses increased at low contrast but remained unchanged at high contrast. This may at first seem inconsistent with the behavioral results. Specifically, behaviorally the sensitivity decreases with size, whereas the BOLD responses in hMT+ remains unchanged instead of also decreasing. We believe that there may be several reasons for this. Firstly, because we were interested in the modulatory effects of the surround on the neurons that were processing the center, we sought to identify regions of cortex that process the part of the visual field that correspond to the position and size of the small stimuli (center). To do this, first we identified the voxels that responded more strongly to 60% contrast small drifting gratings compared to a blank screen. Given the large number of neurons in an fMRI voxel (about a million), and their possible heterogeneity, it is likely that neurons with larger receptive

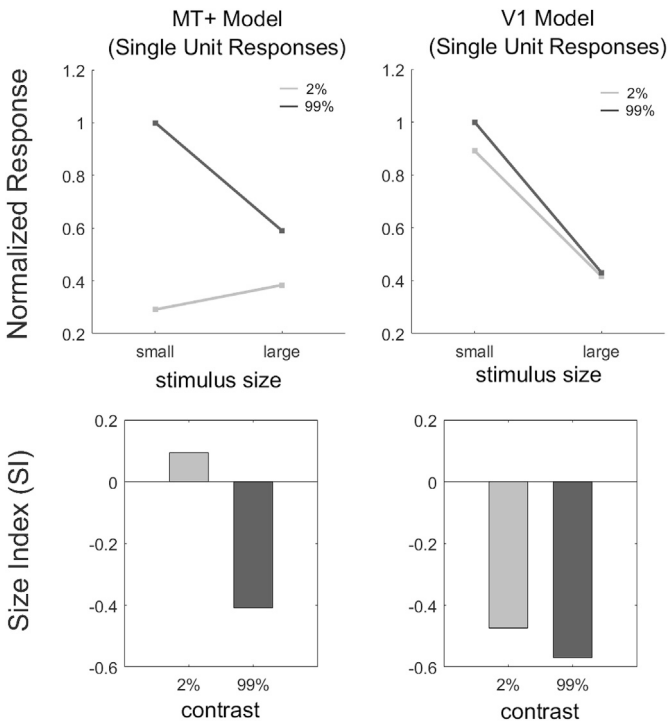

Fig. 7. Divisive normalization model simulations based on single most strongly active unit. MT+ model predictions are largely unchanged compared to the population simulations. They still agree both with our behavioral findings and the pattern of BOLD responses we observed in hMT+. V1 predictions, however, are drastically different, and they do not agree with the BOLD responses we observed in V1, as well as the behavioral effect.

fields that respond directly to both small (center) and large (center + surround) stimuli could have been included in this ROI. This scenario is especially likely in hMT+ where RF sizes are usually much larger. Those neurons could have responded more strongly during the presentation of the large stimulus, muting the effect of response reduction in the neurons that respond only to the center. Indeed when we repeated the analyses within an alternative and more selective ROI, we found suppression for high contrast. For this alternative ROI, we picked the voxels that respond to the center of the stimuli, and at the same time respond more strongly to the small stimulus compared to the large one at high contrast (99%). This allowed us to find a slightly different group of voxels in which suppressed neuronal activity was not muted by increased activity of other neurons. Considering all these, we argue that assessing the neuronal responses using the pattern of Size Indices (*SI*s), not their absolute values, is more appropriate, because *SI* better represents the overall pattern of interaction between size and contrast (e.g. by contrasting *SI* under low and high contrast). Based on the *SI*s, we see that hMT+ activity agree with the perceptual sensitivity irrespective of the approach used to identify the ROIs.

Surround modulation in hMT+ has been previously claimed to underlie the size-contrast interaction in motion perception (Tadin et al., 2003). Two recent neuroimaging results landed support for this hypothesis (Turkozer et al., 2016; Schallmo et al., 2018). Specifically, in both studies, the response patterns in hMT+ were found to reflect the size-contrast interaction. The neuronal activity in hMT+, however, could be inherited from earlier areas, particularly the primary visual cortex (V1). To examine this possibility required investigating the responses in earlier areas. This could not be done previously with fMRI due to methodological limitations. In both studies stimuli were presented at the fovea (Turkozer et al., 2016; Schallmo et al., 2018). This part of the visual field is mapped onto the so-called foveal confluence at the occipital pole, where it is difficult to reliably distinguish V1, V2, and V3 using the standard retinotopic mapping techniques (e.g. Engel et al., 1997). Therefore neither of the previous studies could argue strongly that the size-contrast interaction in motion perception did not originate in earlier visual areas (Turkozer et al., 2016; Schallmo et al., 2018). In the present study we have successfully avoided this limitation by presenting the stimuli at the periphery, which allowed us to confidently localize ROIs in V1, as well as hMT+, and analyze the responses in both areas.

We found strong surround facilitation for both high and low contrast stimuli in V1. This may seem unexpected because surround suppression has been routinely shown in V1 using cell-recording methods on animal models (e.g. Jones et al., 2001; Angelucci and Shushruth, 2013; Angelucci et al., 2017), as well as in some fMRI studies on humans (e.g. Zenger-Landolt and Heeger, 2003; Pihlaja et al., 2008; Nurminen et al., 2009; Nurminen et al., 2013). However, similar to our findings here, Press et al. (2001) reported only facilitation in V1 using flickering checkerboard patterns. Several other studies, meanwhile, reported both suppression and facilitation in early visual cortex under different presentation and attention conditions (Williams et al., 2003; Flevaris and Murray, 2015). These inconsistencies may indicate differences between the methods (i.e. fMRI vs. cell recording, and differences in experimental procedures), as we further elaborate below.

One possible and parsimonious interpretation of our results is that there is indeed no surround suppression in V1 under our experimental protocol. In our protocol, participants were required to perform a demanding fixation task. Such a fixation task limits the spatial attention to the foveal region. Limiting the attention, however, has been argued to reduce the suppressive effect of surround (Reynolds and Heeger, 2009). Thus, in our design owing to the fixation task, surround suppression at the periphery might have become vanishingly small or absent.

In combination with attention, the complex role of eccentricity in mediating surround modulation in V1 might have also led to the observed results. For example surround modulation, particularly at the periphery, may involve not only feedforward connections, but include feedback and horizontal mechanisms, as well (Nurminen and Angelucci, 2014; Nurminen et al., 2018). There is little doubt that as part of a vastly interconnected network V1 receives feedback from other visual areas (Shao and Burkhalter, 1996), including those for motion processing (Hupé et al., 1998; Ponce et al., 2008; Paffen, van der Smagt, te Pas and Verstraten, 2005). Attention, once again, is a major factor mediating such top-down influences (Gilbert and Li, 2013). Specifically eliminating attention might have strongly reduced the top-down influences in peripheral V1. Thus a combination of our design choices, including the attention task at fixation and presenting stimuli at periphery, might have reduced or eliminated surround suppression in V1.

Our model simulations, however, suggest an alternative possibility. In a recent study, Schallmo et al. (2018) argued that a single computational mechanism, namely divisive normalization (Heeger, 1992; Reynolds and Heeger, 2009; Carandini and Heeger, 2012), can successfully account for both surround facilitation and suppression (also see Schallmo et al., 2020). Borrowing and extending this idea, we have also tested how well the divisive normalization model could explain our results. We performed our simulations using two different approaches. First, we simulated the aggregate of responses from a population of units to better reflect the BOLD responses from a voxel. In the other approach, we simulated the response of the most active unit. This kind of "winner take all" approach was previously used in literature and argued to better reflect behavior (Schallmo et al., 2018). We found good agreement between the model and hMT+ responses irrespective of the simulation method.

The model could also predict the V1 BOLD responses using our population response approach, i.e. facilitation at both high and low contrast. However, single unit responses exhibited a completely different pattern, predicting suppression for both low and high contrast gratings. This is indeed biologically plausible because the large stimulus likely falls on the so called far-surround and thus cause suppression at both low and high contrast levels (Angelucci and Shushruth, 2013).

Thus the model simulations suggest an alternative explanation for the V1 findings: there might be suppression in V1 at the single unit level but this suppression is muted by the facilitation observed in other neurons in an fMRI voxel.

Our results in hMT+ agree with the results of the two studies introduced above (Turkozer et al., 2016; Schallmo et al., 2018). Turkozer et al. (2016) did not report results from other visual areas, but Schallmo et al. (2018) found surround suppression for all contrast levels in early visual cortex (EVC) defined as the sum of V1, V2 and V3 in the foveal confluence. This seems to stand in contradiction to our findings. The major difference between our study and Schallmo et al. (2018) was the position of the stimuli (periphery vs. fovea). As discussed earlier, this might have led to a reduced surround suppression at the periphery and caused the difference between the two studies. Besides this, however, owing to the methodological limitations described before, Schallmo et al. (2018) could report only the aggregated activity of V1, V2, and V3 (EVC). Reporting the aggregated activity from EVC, however, may have obscured the facilitation in V1. This is probable, because suppression has been shown to be progressively stronger in V2 and V3 than in V1 (Zenger-Landolt and Heeger, 2003). Alternatively, it might have been possible to observe suppression near fovea with fMRI, because RF sizes of neurons that process that part of the visual field are small, and those neurons sample the space more densely (cortical magnification). In other words, within a single voxel neurons with very similar RF centers sample more uniformly a very small part in the visual space. Thus suppressed neurons might constitute the majority in a single voxel, and the suppressive effect may not be muted as much as in the periphery.

5. Conclusion

Our results provide further evidence that size-contrast interaction in motion perception likely originates in hMT+. V1 activity, based on either empirical BOLD responses or simulations, does not agree with the behavioral effect. Furthermore, our numerical simulations show that the divisive normalization model can predict the fMRI BOLD responses in both hMT+ and V1. In a broader context, our results show that surround modulation and its effects on behavior can be distinct across different components of the human visual system.

Data and code availability statement

The data that support the findings of this study are available at https://doi.org/10.17632/5hpxhzxzjj.2.

Declaration of competing interest

None.

CRediT authorship contribution statement

Gorkem Er: Data curation, Formal analysis, Investigation, Software, Visualization, Writing - original draft, Writing - review & editing. **Zahide Pamir:** Conceptualization, Data curation, Formal analysis, Investigation, Methodology, Software, Visualization, Writing - original draft, Writing - review & editing. **Huseyin Boyaci:** Conceptualization, Investigation, Methodology, Resources, Supervision, Writing - original draft, Writing - review & editing.

Acknowledgments

We thank Michael-Paul Schallmo and his colleagues for letting us use their code for testing the divisive normalization model. We thank Halide Bilge Turkozer for her contribution to designing the experimental paradigm. Author ZP was supported by TÜBİTAK (National Scholarship Program for PhD Students, scholarship id: 2211-E). We are grateful to two anonymous reviewers whose comments helped us substantially improve the manuscript.

Appendix A. Supplementary data

Supplementary data to this article can be found online at https://doi.org/10.1016/j.neuroimage.2020.117084.

References

Albright, T., Desimone, R., 1987. Local precision of visuotopic organization in the middle temporal area (MT) of the macaque. Exp. Brain Res. 65 (3), 582–592.
Amano, K., Wandell, B.A., Dumoulin, S.O., 2009. Visual field maps, population receptive field sizes, and visual field coverage in the human MT+ complex. J. Neurophysiol. 102 (5), 2704–2718.
Angelucci, A., Bijanzadeh, M., Nurminen, L., Federer, F., Merlin, S., Bressloff, P.C., 2017. Circuits and mechanisms for surround modulation in visual cortex. Annu. Rev. Neurosci. 40 (1), 425–451. https://doi.org/10.1146/annurev-neuro-072116-031418.
Angelucci, A., Shushruth, S., 2013. Beyond the classical receptive field: Surround modulation in primary visual cortex. In: Werner, J.S., Chalupa, L.M. (Eds.), The New Visual Neurosciences. The MIT Press, Cambridge,MA, pp. 425–444.
Boynton, G.M., Demb, J.B., Glover, G.H., Heeger, D.J., 1999. Neuronal basis of contrast discrimination. Vis. Res. 39 (2), 257–269. https://doi.org/10.1016/S0042-6989(98)00113-8.
Carandini, M., Heeger, D.J., 2012. Normalization as a canonical neural computation. Nat. Rev. Neurosci. 13 (1), 51–62. https://doi.org/10.1038/nrn3136.
Dukelow, S.P., DeSouza, J.F., Culham, J.C., van den Berg, A.V., Menon, R.S., Vilis, T., 2001. Distinguishing subregions of the human MT+ complex using visual fields and pursuit eye movements. J. Neurophysiol. 86 (4), 1991–2000.
Engel, S.A., Glover, G.H., Wandell, B.A., 1997. Retinotopic organization in human visual cortex and the spatial precision of functional MRI. Cerebr. Cortex 7 (2), 181–192.
Flevaris, A.V., Murray, S.O., 2015. Attention determines contextual enhancement versus suppression in human primary visual cortex. J. Neurosci. 35 (35), 12273–12280.
Gilbert, C.D., Li, W., 2013. Top-down influences on visual processing. Nat. Rev. Neurosci. 14 (5), 350–363. https://doi.org/10.1038/nrn3476.
Heeger, D.J., 1992. Normalization of cell responses in cat striate cortex. Vis. Neurosci. 9 (2), 181–197.
Huk, A.C., Dougherty, R.F., Heeger, D.J., 2002. Retinotopy and functional subdivision of human areas MT and MST. J. Neurosci. 22 (16), 7195–7205.
Hupé, J., James, A., Payne, B., Lomber, S., Girard, P., Bullier, J., 1998. Cortical feedback improves discrimination between figure and background by V1, V2 and V3 neurons. Nature 394, 784–787. https://doi.org/10.1038/29537.
JASP Team, 2018. JASP (Version 0.8.5)[Computer Software]. Retrieved from. https://jasp-stats.org/.
Jones, H., Grieve, K., Wang, W., Sillito, A., 2001. Surround suppression in primate V1. J. Neurophysiol. 86 (4), 2011–2028.
Kingdom, F.A.A., Prins, N., 2010. Psychophysics: A Practical Introduction. Academic Press: an imprint of Elsevier, London.
Nurminen, L., Angelucci, A., 2014. Multiple components of surround modulation in primary visual cortex: Multiple neural circuits with multiple functions? Vis. Res. 104, 47–56. https://doi.org/10.1016/j.visres.2014.08.018.
Nurminen, L., Kilpeläinen, M., Laurinen, P., Vanni, S., 2009. Area summation in human visual system: Psychophysics, fMRI, and modeling. J. Neurophysiol. 102 (5), 2900–2909.
Nurminen, L., Kilpeläinen, M., Vanni, S., 2013. Fovea-periphery axis symmetry of surround modulation in the human visual system. PloS One 8 (2), e57906.
Nurminen, L., Merlin, S., Bijanzadeh, M., Federer, F., Angelucci, A., 2018. Top-down feedback controls spatial summation and response amplitude in primate visual cortex. Nat. Commun. 9, 2281 https://doi.org/10.1038/s41467-018-04500-5.
Paffen, C.L., van der Smagt, M.J., te Pas, S.F., Verstraten, F.A., 2005. Center-surround inhibition and facilitation as a function of size and contrast at multiple levels of visual motion processing. J. Vis. 5 (6), 8 https://doi.org/10.1167/5.6.8.
Peirce, J., 2009. Generating stimuli for neuroscience using Psychopy. Front. Neuroinf. 2, 10. https://doi.org/10.3389/neuro.11.010.2008.
Pihlaja, M., Henriksson, L., James, A.C., Vanni, S., 2008. Quantitative multifocal fMRI shows active suppression in human V1. Hum. Brain Mapp. 29 (9), 1001–1014.
Ponce, C.R., Lomber, S.G., Born, R.T., 2008. Integrating motion and depth via parallel pathways. Nat. Neurosci. 11, 216–223. https://doi.org/10.1038/nn2039.
Press, W.A., Brewer, A.A., Dougherty, R.F., Wade, A.R., Wandell, B.A., 2001. Visual areas and spatial summation in human visual cortex. Vis. Res. 41 (10–11), 1321–1332. https://doi.org/10.1016/S0042-6989(01)00074-8.
Reynolds, J.H., Heeger, D.J., 2009. The normalization model of attention. Neuron 61 (2), 168–185.
Sceniak, M.P., Ringach, D.L., Hawken, M.J., Shapley, R., 1999. Contrast's effect on spatial summation by macaque V1 neurons. Nat. Neurosci. 2, 733–739. https://doi.org/10.1038/11197.
Schallmo, M.P., Kale, A.M., Millin, R., Flevaris, A.V., Brkanac, Z., Edden, R.A., Murray, S.O., 2018. Suppression and facilitation of human neural responses. eLife 7, 1–23. https://doi.org/10.7554/eLife.30334.001.
Schallmo, M., Kolodny, T., Kale, A.M., 2020. Weaker neural suppression in autism. Nat Commun 11. https://doi.org/10.1038/s41467-020-16495-z, 2675.
Shao, Z., Burkhalter, A., 1996. Different balance of excitation and inhibition in forward and feedback circuits of rat visual cortex. J. Neurosci. 16 (22), 7353–7365.

Smith, A., Wall, M., Williams, A., Singh, K.D., 2006. Sensitivity to optic flow in human cortical areas MT and MST. Eur. J. Neurosci. 23 (2), 561–569.
Tadin, D., Lappin, J.S., Gilroy, L.A., Blake, R., 2003. Perceptual consequences of centre-surround antagonism in visual motion processing. Nature 424, 312–315. https://doi.org/10.1038/nature01800.
Tadin, D., Silvanto, J., Pascual-Leone, A., Battelli, L., 2011. Improved motion perception and impaired spatial suppression following disruption of cortical area MT/V5. J. Neurosci. 31 (4), 1279–1283.
Turkozer, H.B., Pamir, Z., Boyaci, H., 2016. Contrast affects fMRI activity in middle temporal cortex related to center–surround interaction in motion perception. Front. Psychol. 7, 454 https://doi.org/10.3389/fpsyg.2016.00454.
Williams, A.L., Singh, K.D., Smith, A.T., 2003. Surround modulation measured with functional MRI in the human visual cortex. J. Neurophysiol. 89 (1), 525–533.
Zenger-Landolt, B., Heeger, D.J., 2003. Response suppression in V1 agrees with psychophysics of surround masking. J. Neurosci. 23 (17), 6884–6893.